

Calibration of ION ABUNDANCE in a TOF-MS Spectrum

Kevin L. Hunter and Richard W. Stresau
ETP Electron Multipliers, Ermington, Australia

Presented at the 46th ASMS Conference on Mass Spectroscopy and Allied Topics
May 31-June 4, 1998, Orlando, Florida

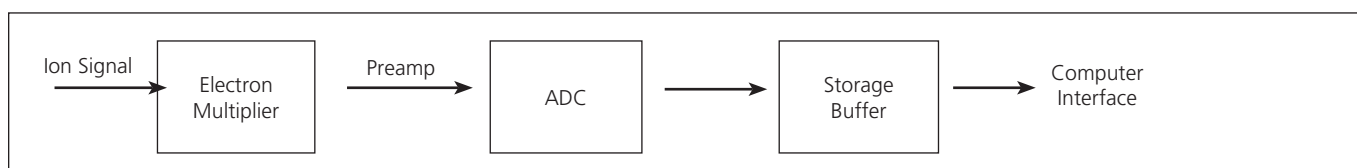


Figure 1. Generalized functional layout of the detection system of a Time of Flight Mass Spectrometer.

INTRODUCTION

Detection systems for TOF mass spectrometers in general make use of an electron-multiplier detector to convert the ion signal into electrons and then to multiply the electron current. This signal is then fed into an Analog-to-Digital-Converter (ADC) to give a digitized form of the signal (Figure 1).

For a multiplier set to a particular average gain (typically 106) the size of the pulse generated in response to an input ion varies according to the multiplier's output pulse-height distribution (Figure 2).

For this type of system, the gain of the multiplier is set so that the threshold level of the first bit of the ADC corresponds to a percentage of the mean pulse size from the multiplier (typically between 10% and 70%) as illustrated in figure 3. For ions that are arriving singly at the detector, the effective detection efficiency is equal to the fraction of input ion events that produce an output pulse above the level of the first bit of the ADC.

For ions arriving simultaneously at the detector in groups (up to 1000's at a time), the sum of the signals generated in the multiplier by each ion will be collected at the multiplier output electrode (figure 4). Here all the pulses are above the level of the first bit of the ADC and the effective detection efficiency is 100%. Consequently the detection efficiency will change with the number of ions being measured in single scan of a mass peak, resulting in a non-linearity in the system with ion abundance.

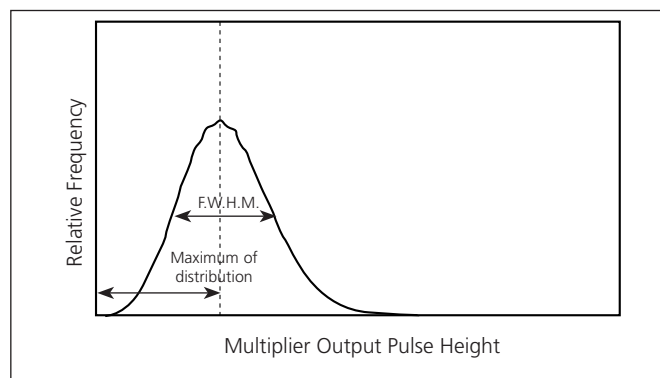


Figure 2. Typical multiplier output pulse height distribution which has a mean pulse height set by the right gain of the multiplier, and a spread described by the Full-Width-at-Half-Maximum (FWHM) of the distribution expressed as a percentage of the peak distribution position.

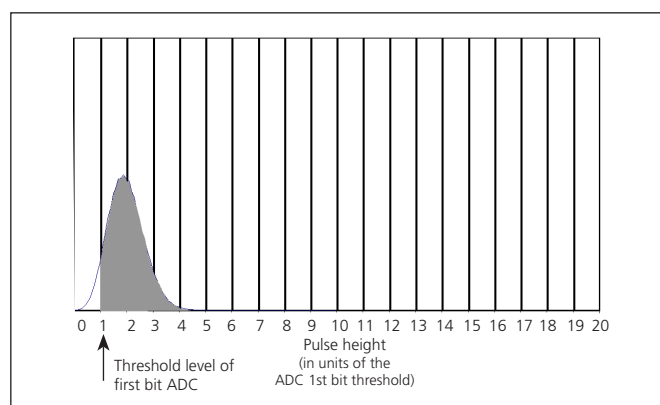


Figure 3. The threshold level of the first bit of the ADC is set at 50% of the mean output pulse height from the multiplier. For ions that are arriving singly at the detector a fraction of input ion events will produce a pulse that falls below the level of the first bit of the ADC.

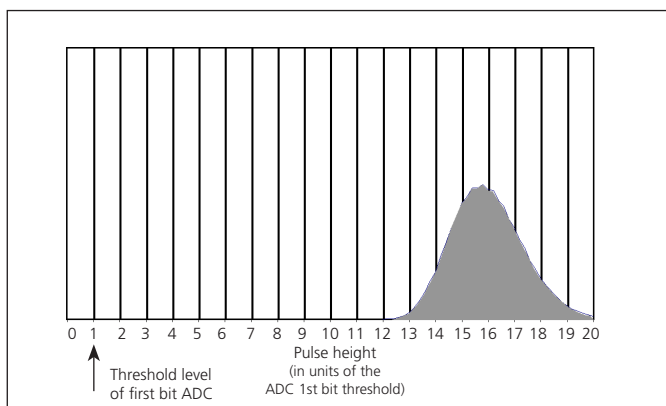


Figure 4. The threshold level of the first bit of the ADC is set to 50% of the mean output pulse height from the multiplier for a single ion. For ions that are arriving at the detector in groups of many (up to 1000's at a time), essentially all the input ion events are counted.

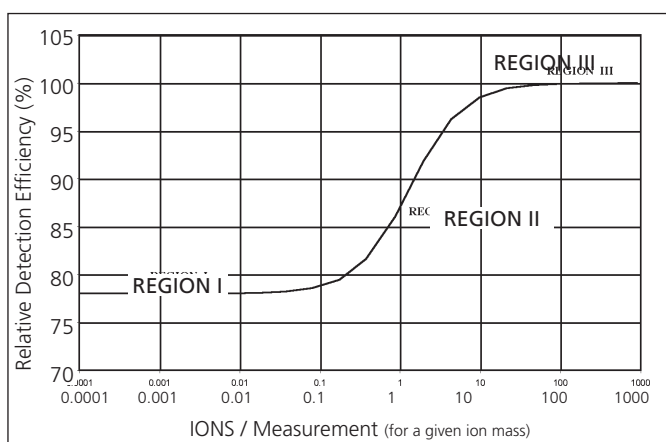


Figure 5. Detection efficiency curve for the TOF detection system. This curve has three distinct regions; Region I (single ions), Region III (groups of many ions), and a transition region, Region II (mix of single ions and larger groups).

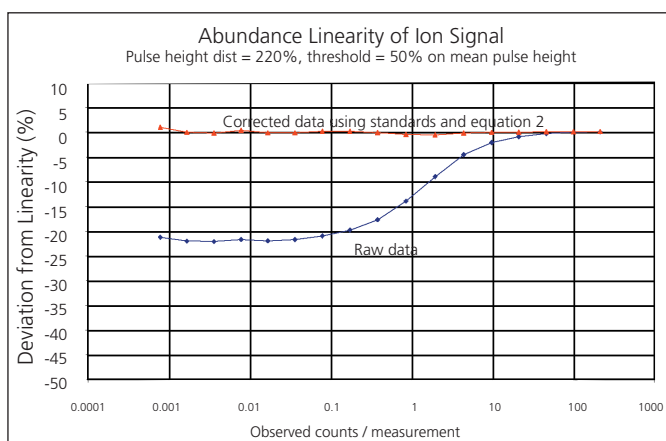


Figure 6. Theoretical results (using Monte-Carlo simulation) for a detection system using an electron multiplier with an output pulse height distribution of FWHM=220% (as a percentage of the peak pulse height) and the threshold level of the 1st bit of the ADC set at 50% of the mean pulse height. The corrected linearity curve was obtained using equation 2 and using the values: A=0.78, B=1.30, C=1.30.

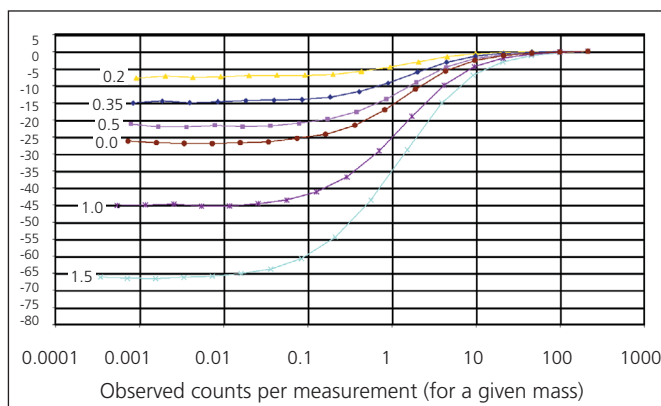


Figure 7. Theoretical results (using Monte-Carlo simulation) for a detection system using an electron multiplier with an output pulse height distribution of FWHM=220%. The threshold level of the 1st bit of the ADC is set at a range of values from 0.2 to 1.5 (expressed as a fraction of the mean pulse height).

CORRECTING THE ABUNDANCE SCALE NON-LINEARITY

Method A: Using Selected Standards and the Functional form of the Calibration Curve.

The calibration curve between the measured ion abundance per measurement, X, and the real number of ions per measurement reaching the detector, Y, is shown in figure 5. The mathematical form of this curve is as follows:

$$X = Y * K \tag{eqn.1}$$

$$\text{where } K = \frac{1.0-A}{2} + \frac{A}{2} \tanh B \log_{10} \frac{X}{C} \tag{eqn.2}$$

And the constants A, B and C are:

- A - low ion-intensity detection efficiency
- B - slope of the inflection region
- C - value of X at the inflection point

By using appropriate calibration samples which give ion peaks on both plateaus and in the transition region of figure 6, the values of A, B and C can be determined. Figure 6 shows theoretical results after the correction of equation 2 was made. The linearity of the system is now within $\pm 1\%$.

Method B: Quantization Correction with appropriate setting of discriminator level

The amount of non-linearity seen in the measured abundance is strongly dependent on the chosen setting for the discriminator level (figure 7). Good linearity can be achieved when the discriminator

setting is a small fraction of the mean pulse height. In practice the minimum discriminator level is limited by line noise. This situation can be improved by correcting the signal from the ADC for the error generated by the digitization of the pulse size (figure 8). This quantization error can be compensated for every time a measurement is taken by applying the expression:

$$\text{Corrected ADC Output} = \text{ADC Output} + 0.5 \text{ (eqn. 3)}$$

Figure 9 shows the same data after using the quantization correction of equation 3. Good linearity is achieved when the threshold level is set to 0.35 (fraction of the mean pulse height). From this result it can be readily seen that the detection system can be calibrated by using a set of standards, with a signal intensity that is on each plateau region, and then adjusting the gain of the multiplier (or the relative value of the threshold of the ADC) until the correct ratio of the two standards is achieved.

Method C: Quantization Correction and Calibration Curve

Alternatively the quantization-corrected data in figure 9 could be further corrected by also applying Method A. In this case the functional form of the corrected data can be used in conjunction with known ion intensity standards to provide calibration of the system.

We have also found that for the quantization-corrected data, the response linearity curves (figure 9) are not as symmetric as those of the raw data (without quantization-correction). Better results are obtained if a different value for the constant B is used in equation 2 for data points with ion intensities greater than the inflection point of the curve.

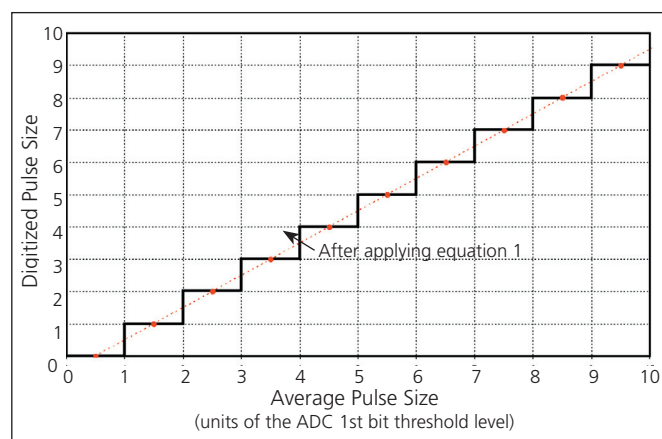


Figure 8. The digitized output of the ADC plotted as a function of the input pulse size. If a group of pulses with heights evenly distributed between the thresholds of the third and fourth bits of the ADC, then the average size of these pulses would be 3.5. However the ADC would read an output of 3 for each pulse.

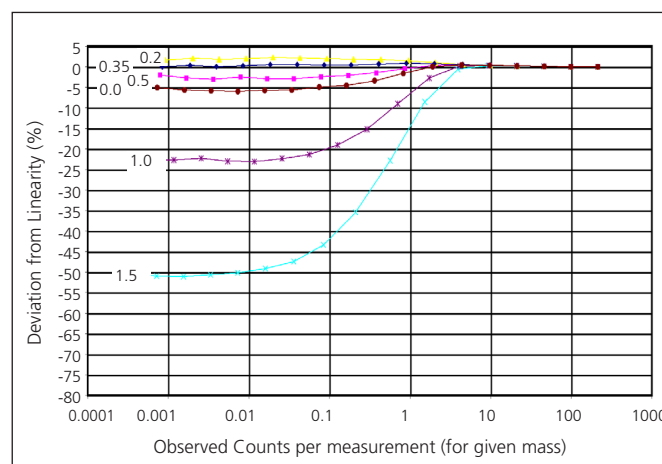


Figure 9. The corrected linearity curves were obtained by applying equation 3 to the data in figure 7. In this case near ideal linearity is achieved when the threshold level of the 1st bit of the ADC is set at a value of 0.35 (expressed as a fraction of the mean pulse height).

CONCLUSIONS

Monte-Carlo methods have proven to be a powerful tool in understanding how ions from a TOF mass spectrometer interact with the electron multiplier and its associated electronics. This study has revealed that serious non-linearities can occur in the measured abundance of ions in a TOF mass spectrum.

Several methods for correcting the non-linearity in the measured ion abundance have been determined;

1. Using selected standards and applying the functional form of the abundance calibration curve determined by this study (equation 2).
2. Applying a quantization correction to the signal from the ADC, and then using standards to select a discriminator level that minimizes the measured abundance non-linearity.
3. Applying a quantization correction to the signal from the ADC. Then using standards and the functional form of the abundance calibration curve (equation 2).



ETP Electron Multipliers

ABN: 35 078 955 521
 Address: 31 Hope Street,
 Melrose Park NSW 2114
 Australia
 Tel: +61 (0)2 8876 0100
 Fax: +61 (0)2 8876 0199
 Email: info@etp-ms.com
 Web: www.etp-ms.com